Novel V-Shaped Negative Temperature Coefficient of Conductivity Thermistors and Electromagnetic Interference Shielding Effectiveness from Butyl Rubber–Loaded Boron Carbide Ceramic Composites

Farid El-Tantawy,[1] Nikolay Dishovsky[2]

[1]*Department of Physics, Faculty of Science, Suez Canal University, Ismailia, Egypt*
[2]*Department of Polymer Engineering, University of Chemical Technology and Metallurgy, 1756 Sofia, Bulgaria*

Received 26 February 2003; accepted 15 July 2003

ABSTRACT: The presentation of a new conductive composite with good effective applications like negative and positive temperature coefficient of conductivity thermistors (i.e., V-shaped thermistors) and electromagnetic interference shielding effectiveness (EMI) was the aim of this study. The effect of boron carbide (B_4C) contents on the vulcanization characteristics and network structure of butyl rubber (IIR) composites were analyzed in detail. The prediction of the type of crosslinks based on the affine and phantom network theory was also analyzed. The influence of the volume fraction of B_4C on the dc conductivity and thermoelectric power was investigated. The electrical and dielectric properties of IIR composites were investigated. The results suggest that the conduction occurs by a tunneling mechanism and behaves as a p-type semiconductor. Isothermal resistance at different temperatures, as a function of B_4C content, was displayed. The current–voltage characteristics showed properties of switches, which were explained by coulombic repulsive force. For practical applications, as self-electrical heating the temperature–time cycles were investigated under certain applied power. It was found that increasing the B_4C content increases the thermal stability of the composite. However, the theoretical modeling of the current–voltage characteristic is very useful for planning groups in industrial applications of conducting polymer composites. Furthermore, the endurance test under applied power indicates that the proposed composites could be useful as temperature sensors with good reliability. Specific heat as a function of B_4C contents was evaluated by experimental and various energy balance models. Furthermore, the temperature dependency of thermal conductivity and thermal diffusivity were investigated. Finally, the standing wave ratio, reflection coefficient, return loss, and attenuation of IIR/B_4C composites were studied in the 1- to 4-GHz frequency range. The resulting values of electromagnetic interference shielding effectiveness were compared with theoretical models. © 2004 Wiley Periodicals, Inc. J Appl Polym Sci 91: 2756–2770, 2004

Key words: conducting polymers; vulcanization; networks; thermal properties; electromagnetic interference shielding

INTRODUCTION

Conducting polymers composites have drawn considerable interest in recent years because of their numerous applications in various electrical and electronic devices. In most of these applications, the main objective is to obtain a sufficient level of electrical conductivity and dielectric constant in the composite.[1] Lately, it has been found that these composites exhibit some novel properties and may be used for the following applications: negative and positive temperature coefficient of conductivity (NTCC/PTCC) thermistors (i.e., V-shaped thermistor), temperature sensors,[1–3] circuit-protection devices,[3] antistatic shielding,[4] electromagnetic interference shielding,[5] typical antenna systems,[6] anechoic chambers designed to avoid interference arising from unwanted electromagnetic field during measurement,[7] radar cross section,[8] computer housing,[9] and different types of pressure-sensitive switches,[10] to cite some of the more prominent uses. In fact, the mechanism behind the NTCC abnormality has not been well established. Generally, the effect of fillers on the electrical properties of rubber is of great interest primarily because fillers can be used very efficiently to change the physical properties. The electrical properties of rubber filled with structured filler are influenced by factors such as type of filler, particle size, volume fraction, surface area of filler, and process condition.[11]

Boron carbide (B_4C) exhibits many attractive properties, such as low specific weight, high chemical stability, high modulus, good wear resistance, and low electrical resistivity at room temperature.[12] The replacement of carbon black by a nonoxide conductive ceramic like B_4C may provide new properties and applications. As the use of electronic products and communication instructions increases, the electromagnetic interference (EMI) shielding effectiveness be-

Correspondence to: F. El-Tantawy (faridtantawy@yahoo.com).

Journal of Applied Polymer Science, Vol. 91, 2756–2770 (2004)

TABLE I
Composition of the Mixes

Ingredient (phr)	F20	F25	F30	F35	F40
IIR	100	100	100	100	100
Stearic acid	3	3	3	3	3
Zinc oxide	6	6	6	6	6
Naphthenic oil	12	12	12	12	12
Boron carbide	20	25	30	35	40
TMTD[a]	1	1	1	1	1
CBS[b]	1	1	1	1	1
PβN[c]	1	1	1	1	1
Styrenated phenol	1	1	1	1	1
Sulfur	1	1	1	1	1
DCP[d]	0.5	0.5	0.5	0.5	0.5
Si-69[e]	0.5	0.5	0.5	0.5	0.5

[a] Tetra methyl thiuranm disulfide.
[b] *N*-Cyclo hexyls benzthiazyl sulphenamide.
[c] Phenyl-β-naphthylamine.
[d] Dicmyl peroxide.
[e] Bis-(3-triethoxysilylpropyl) tetra sulfide.

comes a problem because the lifetime and the efficiency of the instruments and harmful to humans.[3,4] To the author's knowledge, no data have been found in the open literature about the physicochemical properties of butyl rubber (IIR)/B_4C composites. With this consideration, we sought to reinforce IIR with B_4C to obtain new conducting polymer/ceramic composites exhibiting novel properties. In the present article, the effect of B_4C on vulcanization processes, network structure, electrical conducting characteristics, dielectric constant, thermal properties such as thermal conductivity, diffusivity, specific heat capacity, and electromagnetic wave shielding effectiveness are examined.

EXPERIMENTAL

Raw materials and fabrication processing

IIR rubbers were supplied by Japan Synthetic Rubber Co. The boron carbide (B_4C) powder was purchased from Kojundo Chemical Laboratory Co. (Japan), containing boron 77 wt % and carbon 21 wt %, with particle size 2 μm, and used as electrical conductive filler. The various formulations used in this study are proprietary and a general list of ingredients is presented in Table I. A series of IIR/B_4C composites were fabricated by traditional rubber techniques in a two-roll mill (diameter 170 mm, working distance 300 mm, slow speed 18 rpm, and gear ratio 1.33) at a temperature of 40°C. An overall mixing time of 1 h at 40°C was allowed to ensure uniform and efficient dispersion of conductive particles in the rubber matrix. The speed of the front roll was less than the speed of the back roll to prevent bagging of the base polymer; the speed ratio was 1 : 1.4. The mill was operated at 40°C with cold water circulated through the rolls to prevent excessive heat generation during mixing. The compounded rubber was left at least 24 h before vulcanization. The vulcanization of the rubber composites was carried out in an electrically heated press between stainless-steel platens at a temperature of 160°C and under a pressure of about 500 kN/m^2 for dwelling time of 1 h. A thin brass electrode was embedded into samples during the vulcanization process to minimize the contact resistance.[3]

Techniques of characterization

Experimental details of in-line dc electrical conductivity measurements during the vulcanization process were the same as those reported previously.[2] The temperature of the samples was increased from 20 to 160°C at a heating rate of 10°C/min. Scanning electron microscopy (SEM) was used to investigate the surface morphology of the IIR composites after the vulcanization process. Surfaces of the test samples were carefully cut, mounted on an SEM stub using double-sided carbon tape, sputter-coated with gold, and then examined under an electron microscope (model JSM-5310, JEOL, Tokyo, Japan), operated at 20 kV. The density of the composite (ρ_m) was measured by Archimedes technique.[4] The bulk electrical conductivity (σ) was measured using a Multi-Mega–Ohmmeter type MOM12 and a measuring cell ODW2 (from WTW Co., Germany). The data were automatically collected using a suitable interface and data acquisition pc code. The dielectric constant of the composites was measured at frequencies of 1 kHz using an RLC Bridge (3535 Z-Hitester, Hioki, Japan). The data were automatically collected using a suitable interface and data acquisition pc code.

The thermoelectric power (TEP) and/or Seebeck coefficient were measured by using the equation: TEP $= \Delta V/\Delta T$, where ΔV is the thermoelectromotive force produced across the pellet arising from the temperature difference $\Delta T = 10$°C. From TEP and σ, the power factor (PF) was calculated. The determination of the thermal properties, that is, thermal conductivity (λ), thermal diffusivity (K_d), and specific heat (C_p) of the samples was carried out by use of a differential scanning calorimeter (Perkin–Elmer DSC-2; Perkin Elmer Cetus Instruments, Norwalk, CT) using sapphire as the reference material. The K_d was calculated from λ by the following equation: $K_d = 1/\rho_r C_p$, where ρ_r is the density of rubber composite. The EMI properties were determined by a Hewlett–Packard (Palo Alto, CA) waveguide line containing spectroanalyzer, power meter, coefficient of reflection meter, and coefficient of attenuation meter.[5] The measurements were carried out in the frequency range 1.0–4.0 GHz. Hardness was determined using a universal testing machine. The samples were prepared according to the ASTM DIN 2240 standard.[3]

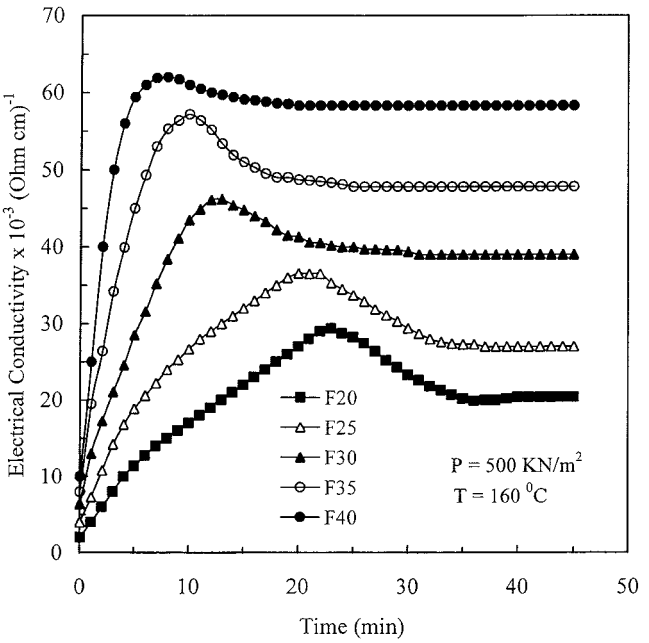

Figure 1 Variation in dc electrical conductivity during vulcanization versus time at 160°C temperature under 500 kN/m^2 pressure for IIR/B_4C composites.

RESULTS AND DISCUSSION

Effect of B_4C on the vulcanization processes

Knowledge of the vulcanization kinetics of conductive polymer composites is essential to choose a proper set of processing parameters and ingredients, which should give good material properties to composites. The variations in dc conductivity during vulcanization versus time at 160°C temperature under 500 kN/m^2 pressure for IIR composites are plotted in Figure 1. It is clearly seen that the vulcanization behaviors of all tested samples are similar but not identical. In Figure 1 behavior of the vulcanization process can be divided into three stages: (1) The conductivity increases rapidly, which is attributed to the ordering of conductive particles and/or aggregates and thermal activation that causes rapid crosslinking density, resulting in a narrow gap distance between conductive particles that can induce high conductivity.[2] (2) The conductivity decreases because of fragmentation of soft conductive particles and formation of particles cluster around aggregates. This phenomenon is believed to be a result of the separation of the conducting particles attributed to the thermal expansion of the polymer. As the filler particles move apart the existing conducting pathways are broken, thus causing a decrease in conductivity. (3) The conductivity increases slightly and then levels off. The slight increase of conductivity again is attributed to the rearrangement of B_4C particles taking place during the vulcanization process, leading to formation of more conductive networks filaments and/or reaccumulation of B_4C at the interface of rubber layers that reduce the gap width by increasing the number of contact nodes as confirmed later in this article. Moreover, we believe that some oxidative structures, resulting from the free electron pairs in collaboration with the polar site present at the B_4C, led to the increase of conductivity. After a certain time, depending on B_4C contents, the conductivity level turns off. This phenomena can be explained by the notion that the conductivity is relatively insensitive to B_4C concentration because of extensive interparticle contacts (i.e., tight neck) and formation of hard rigid aggregates.

In Figure 1, the characteristic vulcanization time constant (τ_V) as a function of B_4C content can be estimated by the following formula and is calculated at time $t = \tau_V$:

$$(\sigma - \sigma_{t=0}) = (\sigma_m - \sigma_{t=0})\left[1 - \exp\left(-\frac{t}{\tau_V}\right)\right] \quad (1)$$

where σ_m and $\sigma_{t=0}$ are the maximum and initial conductivity of the tested samples, respectively.

The calculated values of τ_V as a function of B_4C contents are listed in Table II. It is clear that the τ_V value decreases with increasing B_4C content and the

TABLE II
Some Physical Parameters of IIR/B_4C Composites

Parameter	F20	F25	F30	F35	F40
τ_V (min)	33.21	25.33	17.46	10.27	6.63
CD (g/cm^3)	1.65	1.77	1.86	1.97	2.08
IPD (Å)	200	164	129	89	56
V_r	0.42	0.48	0.55	0.61	0.67
γ	0.83	0.87	0.92	0.97	0.99
VF (%)	70.60	82.30	90.10	96.60	99.20
DS_E	238.09	208.33	181.82	163.93	149.25
M_c					
Experimental	2270	1950	1690	1391	1122
Affine	2110	1810	1560	1301	1091
Phantom	1071	811	689	543	418
CLD $\times$ 10^4 (g/cm^3)	2.20	2.56	2.96	3.59	4.46

optimum curing level is achieved at a time up to 6.63 min. It indicates that B_4C accelerates the curing kinetics and enhances the inner structure cores into the IIR matrix as confirmed later by network structure results.

Effect of B_4C on the network structure

The use of polymer composites in high-temperature industrial technologies requires a thorough knowledge of their network structure. Technological processes of production can be better controlled when the relationship between network structure and the compositions of green input materials is known. The composite density (CD) of IIR filled with B_4C particles is given by the following equation:

$$\mathrm{CD} = \left(\frac{w_0 w_1}{w_2}\right) \tag{2}$$

where w_0 the dry weight of the sample, w_1 is the corrected density of water, and w_2 is the weight of the composite in water.

The interparticle distance between conductive particles (IPD) is calculated according to the equation

$$\mathrm{IPD} = -D\left[\left(\frac{k\pi}{6V_r}\right)^{1/3} - 1\right] \tag{3}$$

where D is the B_4C particle diameter, $k = 1$ (for cubic packing), and V_r is the volume fraction of rubber network and is given by[2]

$$\left(\frac{1}{V_r}\right) = 1 + \left(\frac{\omega_3 \rho_r}{w_0 \rho_s}\right) \tag{4}$$

where ω_3 is the weight of absorbed solvent and ρ_s is the density of the solvent.

The degree of reinforcement depends on the extent of rubber–filler interaction, from which the extent of B_4C reinforcement (γ) on IIR composites can be determined as[4]

$$\left(\frac{V_r}{V_{r0}}\right) = 1 - \gamma\left(\frac{\beta}{1-\beta}\right) \tag{5}$$

where V_{r0} is the volume fraction of rubber in the filled vulcanizate and β is the content of B_4C.

The vulcanization fraction (VF) was determined by soaking the test samples in kerosene for 30 h, after which the samples were dried to a constant weight in vacuum at 50°C. The insoluble fraction was calculated as the ratio of mass loss and initial mass by use of the following equation:

$$\mathrm{VF}\ (\%) = \left(\frac{\omega_4}{w_0}\right) \times 100 \tag{6}$$

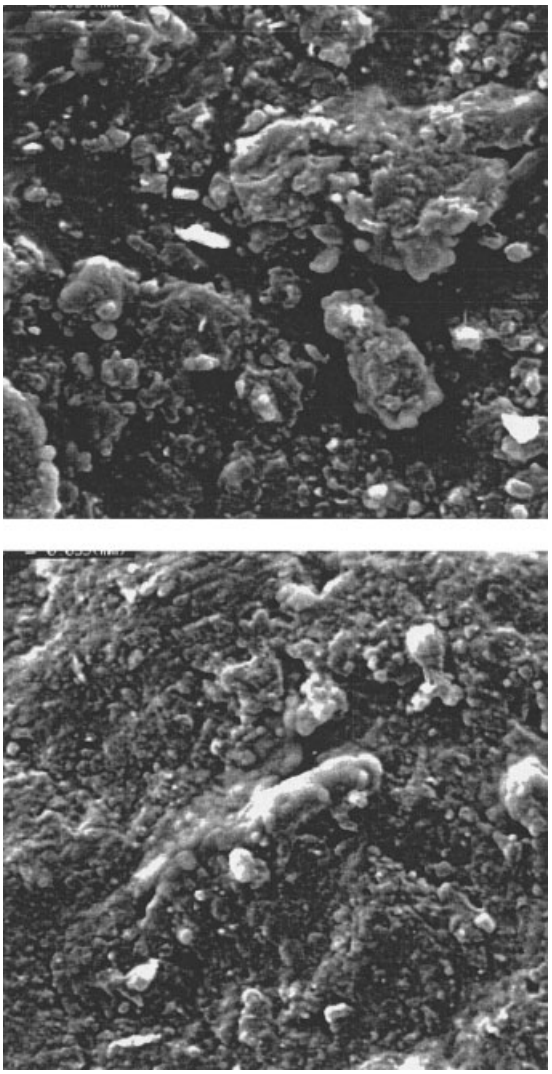

Figure 2 SEM micrographs of (a) sample F20 and (b) sample F40.

where ω_4 is the weight of insoluble portion of the sample.

The calculated values of CD, IPD, V_r, γ, and VF as a function of B_4C are listed in Table II. It is very clear that IPD decreases whereas CD, V_r, γ, and VF increase with increasing B_4C content. These advantages were attributed to the well-developed composite network structure by the incorporation of B_4C, which resulted in a more homogeneous microstructure of composite, as confirmed by SEM [Fig. 2(a), (b)]. This reflects that B_4C increases the crosslinking density and interfacial interactions within the rubber matrix.

However, the average molecular weight between crosslinks (M_c) can be determined by the Flory–Rehner equation[2]:

$$M_c = \frac{(\rho_r V_k)(DS_E^{-1/3} - 1/2DS_E^{-1})}{\ln(1 - DS_E^{-1}) + DS_E^{-1} + \chi DS_E^{-1}} \tag{7}$$

where V_k is the molar volume of kerosene and DS_E is the equilibrium degree of swelling, given as

$$DS_E = 1 + \left(\frac{\rho_r}{\rho_s}\right)\left(\frac{\omega_5}{w_0 - 1}\right) \quad (8)$$

where ω_5 is the weight of sample after swelling in kerosene for 24 h and χ is the polymer–solvent interaction parameter and is calculated from the values of DS_E using the equation

$$\chi = 0.431 - 0.311DS_E^{-1} - 0.036DS_E^{-2} \quad (9)$$

The calculated values of DS_E as a function of B_4C content are listed in Table II for the IIR/B_4C composites. The variation of DS_E depends on the composite composition (i.e., B_4C content). The decrease of DS_E with increasing B_4C content confirms that B_4C enhances the interfacial adhesion and chain connectivity within the rubber matrix.

According to the affine and phantom network models the molecular weight between physical crosslinks is given by[1,3]

$$M_c \text{ (affine)} = \frac{(\rho_r V_k V_r)\left(1 - \frac{\mu}{\phi_1} V_r^{1/3}\right)}{-[\ln(1 - V_r) + V_r + \chi V_r^2]} \quad (10)$$

$$M_c \text{ (phantom)} = \frac{(\rho_r V_k V_r)\left(1 - \frac{2}{\theta}\right)}{-[\ln(1 - V_r) + V_r + \chi V_r^2]} \quad (11)$$

where μ is the number of effective network chains/cm^3 of crosslinked polymer (chain density and/or network density), θ is the junction functionality or number of chains emanating from each crosslink (usually assumed to be 4), and ϕ_1 is the number of junctions, given as $\phi_1 = 1 - (2/\theta)$.

The values of molecular weight—experimental M_c (exp), M_c (affine), and M_c (phantom)—as a function of B_4C contents of IIR composites are listed in Table II. From a comparison between the three values of molecular weight, it may be seen that the experimental values are close to the affine model and far from the phantom model. These imply that the crosslinking junctions are embedded in the network and cannot fluctuate freely, and the chain vector transforms linearly with macroscopic deformation.[2]

Finally, the crosslinking density (CLD) is determined by the following equation:

$$\text{CLD} = \frac{1}{2}\left(\frac{\rho_r N_A}{M_{c(\text{exp})}}\right) \quad (12)$$

where N_A is Avogadro's number.

The values of CLD as a function of B_4C contents are listed in Table II, from which it may be seen that the higher the B_4C content, the higher the CLD of the composite. This fact means that the chain connectivity increases with increasing B_4C content in the matrix as confirmed by SEM micrographs.

Morphological studies

The morphology of the vulcanized samples was assessed by SEM. Figure 2(a) and (b) show the morphology of the IIR/B_4C composite for samples F20 and F40, respectively. In comparison, the morphologies of rubber composites are different depending on B_4C content. Use of 20 wt % B_4C gives nonhomogeneous distribution of conductive particles inside the rubber matrix, which reflects the increase of the gap width among conductive particles of the matrix. On the other hand, use of 40 wt % B_4C gives a good connectivity among conductive particles and the dispersion of the B_4C particles was relatively homogeneous in most areas of the matrix. Also the contiguity of the B_4C particles appears to be enhanced by the increase in volume fraction and most of the B_4C particles are located at the polymer interfaces. It is evident from SEM that the increased interface interaction between filler and matrix results in a high composite conductivity, dielectric constant, thermal conductivity, and electromagnetic shielding effectiveness as confirmed later in this article.

Static electrical conductivity

The static electrical conductivity of IIR composite as a function of B_4C contents is plotted in Figure 3(a), from which it may be seen that there is a substantial increase in conductivity with the increase of B_4C concentration. This behavior may be explained as follows: at a low content of B_4C, the electrical properties were dominated by the polymer phase between the aggregates. Thus, the conductivity of the conductive rubber composite is slightly lowered because of the insulation of rubber matrix on B_4C particles. In other words, the separation distance between B_4C particles is relatively large; the first addition of B_4C ceramic starts to partially fill the free volume inside the rubber matrix. Hence, the further addition of B_4C decreases the interspacing distance and the latter forms discrete chains and new conductive paths. This leads to an increase of the physical contact among conductive particles and forms a three-dimensional network structure that results in an increase of electrical conductivity.

The percolation threshold β_t value of the conducting composite is about 0.17 wt % of B_4C, which is much lower than that of conventional conducting composites.[12,14] This may be because the B_4C decreases the

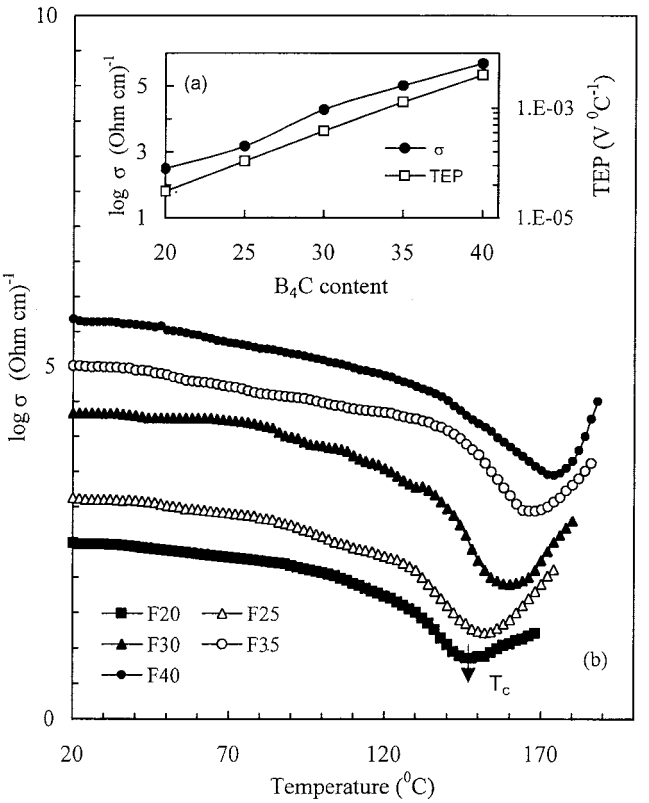

Figure 3 (a) Static electrical conductivity and TEP as a function of B_4C content. (b) Temperature dependency of conductivity of IIR/B_4C composites.

shearing force of the IIR matrix that helps in the formation of continuous conductive paths, as confirmed by the measured hardness against B_4C content in Table III. However, the faster formation of conductive networks throughout the IIR matrix leads to a lower filler content (i.e., lower β_t) and a linear increase in conductivity. It is worth noting that the IIR/B_4C composites exhibit linear conductivity behavior that could be controlled using B_4C particles for any desirable utilization technology.

The bulk conductivity of the composite (σ) at volume content (β) follows a power law equation:

$$\sigma = \sigma_s(\beta - \beta_t)^Y \tag{13}$$

where σ_s is a scale factor and Y is an exponent and/or geometric factor.

The calculated value of Y is about 1.8. This value indicates good interfacial adhesion between the rubber and filler, as confirmed by SEM analysis.

The backing factor (B_F) of conductive particles is related to the β_t by the following equations[5]:

$$B_F = \left(\frac{\beta_c}{\beta_t}\right) \quad \text{and} \quad \beta_t = \left(\frac{B_F}{Z_{\text{eff}}}\right) \tag{14}$$

where β_c is the critical value of the volume fraction after percolation (which creates a sharp change in electrical conductivity) and Z_{eff} is the effective coordination number.

The values of B_F and Z_{eff} are 1.11 and 6.53, respectively. These values indicate that the density of charge carriers increases with increasing B_4C particle content in the composite. Moreover, the B_4C particles arranged themselves in the form of closely packed clusters within the rubber matrix and the trend of the percolation was bound percolation.[3]

Seebeck coefficient (TEP) and power factor (PF)

TEP is one of the important electrical properties for judging the conduction mechanism of conductive materials and allows direct conversion of thermal energy into electrical energy. Figure 3(a) shows the TEP against B_4C content of IIR composites. From Figure 3(a), it may be seen that the TEP increases with increasing B_4C content. This indicates that B_4C modified the macroscopic structure (i.e., increased the network structure density) of the rubber matrix. In addition, the TEP values are positive, showing a p-type semiconductor, and the characteristic of charge is transported by holes. It is interesting to note that the values of TEP are high for IIR/B_4C composites compared to those of conventional composites.[13] This indicates that the proposed composites are very favorable candidates for thermoelectric energy conversion and thermoelectric devices. The power factors (PF) as a function of B_4C content are listed in Table III, from which it may be seen that the PF increased with increasing B_4C content in the composites. This might be attributable to the increase of crosslinking density and thermal stability of the rubber matrix with increasing B_4C content.

A general expression for TEP is given by the following equation[14]:

$$\text{TEP} = \pm \frac{K_B}{e}\left(\frac{E - E_F}{K_B T} + F\right) \tag{15}$$

where e is the elemental charge, E is the position of the energy level of conduction, E_F is the Fermi energy in the samples, K_B is the Boltzmann constant, T is the absolute temperature, and F is a constant between 2 and 4 depending on the scattering mechanism in the material.

The calculated values of $\Delta E = E - E_F$ as a function of B_4C contents are recorded in Table III. The position of the Fermi level in the sample at about 0.123 eV, which is the lowest occupied molecular level, falls into the typical range for semiconductor material of p-type conductivity.[15] This means that the charge carriers have to overcome a considerable barrier in their trans-

TABLE III
Some Physical Parameters of IIR/B_4C Composites

Parameter	F20	F25	F30	F35	F40
Hardness (shore A)	39	44	51	57	64
PF $\times 10^{-5}$ (W m^{-1} K^{-2})	1.23	2.28	3.30	4.35	6.41
$\Delta E = E - E_f$ (eV)	0.123	0.128	0.130	0.135	0.141
SF $\times 10^{-10}$ (Newton)	1.75	1.38	1.05	0.71	0.43
AF $\times 10^{-10}$ (Newton)	2.11	1.63	1.27	0.94	0.63
NTCC $\times 10^2$ (°C^{-1})	−5.483	−4.421	−3.231	−1.972	−0.711
PTCC $\times 10^2$ (°C^{-1})	3.265	4.874	5.973	6.881	7.786
δ	0.83	0.69	0.62	0.51	0.38
T_{LW} (K)	34,887	23,009	12,872	8835	4869
E_a (eV)	0.95	0.78	0.59	0.41	0.21
E_h (eV)	1.60	1.31	0.98	0.71	0.40
G (nm)	9.01	7.21	5.15	3.40	1.91
$N(E) \times 10^{22}$ (cm^{-3})	3.41	6.32	8.51	10.11	11.09
τ_R (min^{-1})					
at 70°C	22	17	12	8	5
at 100°C	24	20	15	12	9
at 130°C	28	23	19	15	12
τ_i (min^{-1})	13	11	9	7	5
τ_g (min^{-1})	12	9	7	5	3
τ_c (min^{-1})	11	10	7	5	4
H_r (J m^{-2} s^{-1} °C^{-1})	52	63	70	79	86
C_p (J kg^{-1} °C^{-1})					
Measuring	3.39	3.51	3.62	3.74	3.81
Conservation	3.45	3.60	3.64	3.80	3.86
Newton	3.40	3.48	3.60	3.77	3.83
Adiabatic	3.42	3.50	3.61	3.71	3.80
$Z \times 10^{-2}$ K^{-1}	2.11	3.26	4.87	5.23	6.83
SD (nm)	0.0036	0.0076	0.0136	0.0234	0.0375

port, which supports a tunneling mechanism (as confirmed later in this article).

Electrical conductivity versus temperature characteristics

The electrical transport properties of the rubber composites are of great importance in determining whether the composite is congruent with our requirements for technological applications. In fact, the effect of temperature on IIR/B_4C composites is quite complex. The temperature dependency on the conductivity of IIR/B_4C composites is depicted in Figure 3(b). It may be observed that at a relatively low temperature range (20–50°C), the conductivity slightly decreases dependent on B_4C contents. This may be attributed to the direct contact of B_4C particles that resist the breakage as the rubber is thermally expanded. At moderate temperatures, the conductivity decreases with the increase of temperature and shows the NTCC effect. This is probably a result of the breakdown of B_4C structures attributed to the thermal expansion of the rubber matrix. In other words, the rise of temperature will cause an appreciable increase in the separation distance between B_4C particles. When the separation distance between particles is large enough, the tunneling probability vanishes, which may be the result of the scattering of electrons at the rubber layers between B_4C particles.[3] At relatively high temperature [i.e., percolation temperature, T_c; see Fig. 3(b)], the conductivity increases again and shows the PTCC effect. The PTCC effect is attributed mainly to two reasons: (1) at T_c the separation distance between B_4C particles becomes so large, simultaneously, the intrinsic conduction attributed to the carriers of the host materials begins to appear; and (2) the diffusion of charge carriers decreases at high temperature because of the increase of viscosity and decrease of the surface energy of the rubber matrix.[1,4] The increase of viscosity and the decrease of surface energy lead to an increase of the compact swelling attributed to the formation of rich liquid phase, thus creating a new stress—swelling stress—in the polymer matrix. This swelling stress increases the anisotropic and surface energy of conductive filler changes, so the conductive networks will be pushed apart from each other, forming a thin screen and/or membrane barrier within the rubber matrix and therefore PTCC appears.[15]

To confirm this assumption, the swelling force (SF) between conductive particles was calculated and is given by[3]

$$\mathrm{SF} = \frac{(IPD)^2 V_r(\rho_r - \rho_m)RT}{M_R} \tag{16}$$

where ρ_m is the density of composite at melting temperatures, R is the gas constant, and M_R is the molecular weight of rubber.

The calculated values of SF at 125°C as a function of B_4C contents are listed in Table III. On the other hand, the attractive force (AF) between the conductive phases can be defined as[2]

$$\mathrm{AF} = \frac{6a}{(IPD)^2} \tag{17}$$

where a is a property constant.

The calculated values of SF and AF as a function of B_4C contents are listed in Table III. In comparison between the calculated values of SF and AF, it is reasonable to suggest that the SF increased the widening among conductive paths and degraded the conductive network paths in the rubber matrix. This supports that at T_c the SF acts as a hard membrane shield and/or degradation source and then the conductivity abruptly increases. This is why the NTCC abruptly increased with the increase of temperature. The higher the temperature was, the larger the intergranular barriers were. Finally, it is worth mentioning that the bottom of the valleylike depression in the conductivity curve in Figure 3(b) was shifted toward the higher temperature depending on B_4C contents. Therefore we must consider that the presence of the filler into the rubber matrix leads to an increase in crosslinking density and thermodynamic stability of the composites.

Determination of NTCC/PTCC

NTCC/PTCC is the one of the important parameters governing the variation of electrical conductivity with temperature and is given by the following equation[16]:

$$\mathrm{NTCC/PTCC} = \pm \frac{1}{\sigma_0}\left(\frac{d\sigma}{dT}\right) \tag{18}$$

The computed values of NTCC and PTCC as a function of B_4C contents are listed in Table III. The decrease of NTCC and the increase of PTCC with the increase of B_4C contents indicate that B_4C enhances the thermal stability and isotropic structure of the rubber matrix as confirmed above.

Electrical conduction mechanism and activation energy

The temperature dependency of electrical conductivity follows the variable range hopping (VRH) conduction:[17]

$$\sigma(T) = C \exp\left[-\left(\frac{T_{LW}}{T}\right)^{\delta}\right] \tag{19}$$

where C is usually taken as having a much weaker temperature dependency than the exponential term; and T_{LW} is a parameter depending (inversely) on the localization length of the localized electronic wave functions and on the density of states near the Fermi level and $\delta = 1/(1 + d)$, where d is the dimensionality of the hopping.

To determine the VRH exponent δ explicitly, we calculated the reduced activation energy defined as

$$W(T) = -T\frac{d[\ln \sigma(T)]}{d(T)} \tag{20}$$

By using eq. (20) we obtain

$$\log_{10}W(T) = F - \delta \log_{10}T \tag{21}$$

where $F = \delta \log_{10}(T_0) + \log_{10}\delta$.

One can determine δ from the slope in a plot of $\log_{10}W$ against $\log_{10}T$. The calculated values of δ and T_{LW} as a function of B_4C contents are listed in Table III. It is clear that the systematic decrease of δ and T_{LW} with the increase of B_4C contents indicates that the B_4C particles reduced the binding energy between conductive phases and built three-dimensional structural channels into the rubber matrix. For further confirmation, the barrier height energy (E_h) at the domain boundaries and the activation energy (E_a) could be obtained by a least-squares fit to the following equations:

$$\sigma = \frac{\sigma_1}{\sqrt{T}} \exp\left(\frac{-E_h}{KT}\right) \tag{22}$$

$$\sigma = \sigma_2 \exp\left(\frac{-E_a}{KT}\right) \tag{23}$$

where σ_1 and σ_2 are the preexponential factors.

From this fitting, the conduction parameters such as E_a and E_h were estimated as a function of B_4C contents and are listed in Table III, from which it may be seen that as the B_4C content increases there is a decrease in activation and barrier height energies. This evidence confirms that the B_4C particles increase the contacts between conductive phases. It is of interest to note that the values of E_a and E_h are not close. This indicates that the conduction mechanism of conductivity of IIR/B_4C composites is controlled by the tunneling mechanisms into the rubber matrix as confirmed by previous TEP results.

However, the tunneling distance (G) is given by the following equation[4]:

$$G = \left(\frac{9}{8\pi\alpha KTN(E)}\right)^{1/4} \tag{24}$$

where α is the inverse rate of fall of the wave function and is about 17 Å and $N(E)$ is the density of states at the Fermi level, given by

$$N(E) = \frac{\lambda \alpha^3}{KT_0} \tag{25}$$

where $\lambda \approx 18.1$ is a dimensionless constant.

In Table III the calculated values for G and $N(E)$ for IIR/B_4C composites are shown. From Table III we notice that $N(E)$ increases, whereas G decreases with the increase of B_4C contents. This argument indicates that the B_4C acts as a carrier reservoir and increases the density of conductive paths within the rubber matrix. Thus, the increase in the $N(E)$ with increase of B_4C content may be another reason for the decrease in E_a and increase in the bulk composite electrical conductivity.

Isothermal resistance checking

One of the most claimed important advantages of conductive rubber composites is their stability and robustness during thermal conditions. One of the aspects regarding the stability of the composite NTCC/PTCC thermisitors under isothermal conditions was considered. Measurements of dynamic resistivity (i.e., isothermal resistance relaxation with time) provided additional information about the stability and helped further our understanding of the mechanism behind the electrical properties of polymer composites.[3,4] Figure 4(a)–(c) shows the isothermal resistance changes with time at constant temperature of 70, 100, and 130°C, respectively, of IIR/B_4C composites. It may be seen that at first the resistance undergoes a sudden increase followed by a decrease in resistance with time, after which it levels off depending on the B_4C contents. We believe that the volume expansion undergoes a quick change at the beginning of the isothermal course after which it levels off. Therefore, the sudden increase of resistance in the beginning is ascribed to a rapid increase of volume expansion of the rubber matrix. It seems the time for the resistance to reach the maximum is shorter as the isothermal temperature is higher, and when the B_4C contents increase, the samples are more stable. This can be explained that at low contents of B_4C, the slow diffusion of B_4C particles occurs from one grain site to another, which changes the charge distribution. This change in the charge distribution will change the effective carrier density and hence the composite resistivity. This argument confirms that the interfacial adhesion and connectivity between IIR moieties increases with the increase of B_4C contents.

The resistance time relaxation curves may be described by the following equation:

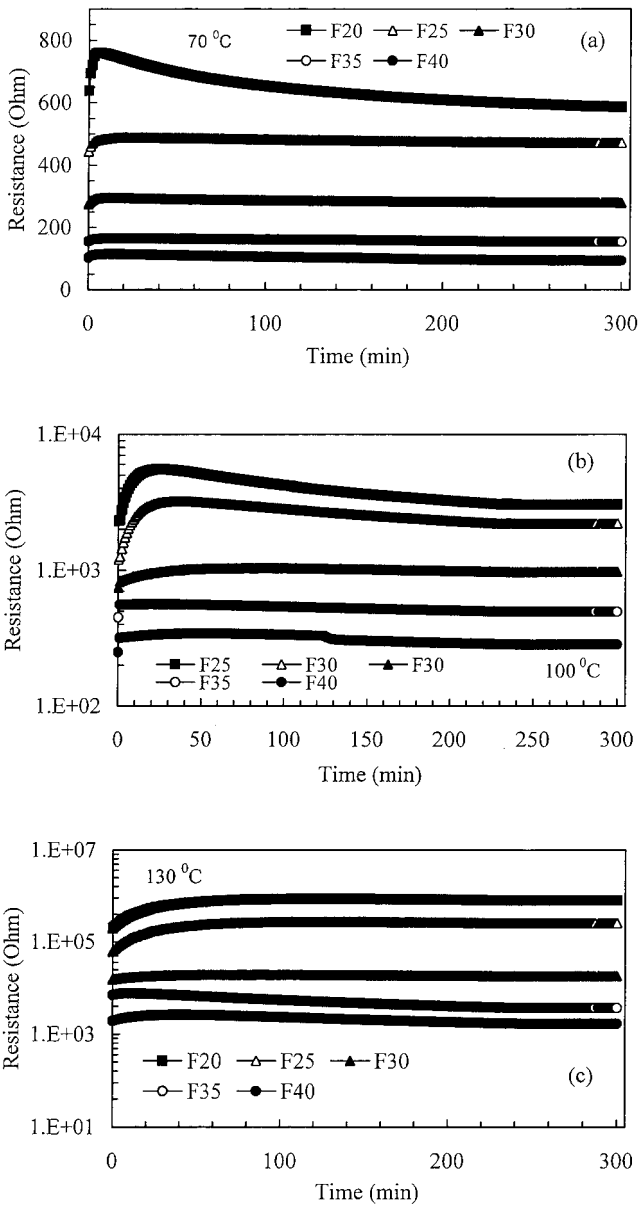

Figure 4 Isothermal resistance changes with time at constant temperature of: (a) 70°C, (b) 100°C, and (c) 130°C, respectively, of IIR/B_4C composites.

$$R(t) = R_0 \exp\left(-\frac{t}{\tau_R}\right) \tag{26}$$

where τ_R is the resistance decay parameter (min^{-1}) and depends on B_4C contents.

The calculated values of τ_R against B_4C contents at various temperatures are listed in Table III, where the decrease of τ_R with increasing B_4C concentration may be interpreted as the increase of the crosslinking density and thermodynamic stability of the composites as confirmed above.

Current–voltage–temperature characteristic

Current switches are very attractive for electronic devices. Also, a switched effect enables conductive com-

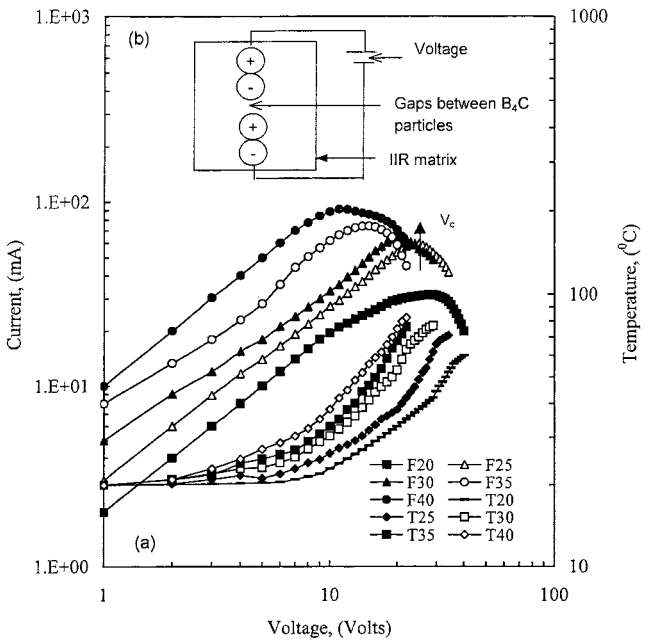

Figure 5 (a) Current–voltage–temperature characteristic of IIR/B_4C composites. (b) Electrical equivalent circuit of conductive particles inside rubber matrix.

posites to perform multiple functions by operating over several voltages. Figure 5(a) shows the variation of current (I) and temperature (T) with voltage (V) for IIR/B_4C composites. It may be seen that the I–V characteristics are linear at low applied voltage without any remarkable change of the sample temperature, indicating the tunneling of electrons on the application of voltage.[1,16] Increasing the electric field above a certain value depends on B_4C contents, leading to an increase in the Joule heating effect and consequently an increase in the bulk sample temperature. Therefore I–V characteristics deviate from linear to nonlinear behavior. By increasing the electric field to a certain value [i.e., switching voltage (V_c); see Fig. 5(a)], which depends on B_4C contents, the current decreases and shows negative resistance (i.e., switching effect). To clarify the switching effect behavior attributed to Joule heating, let us consider the electrical operation circuit of conductive particles inside the rubber matrix that is described by the electric equivalent circuit in Figure 5(b). We speculate that at high electric field (i.e., Joule heating) the whole polymer matrix is heated by Joule heating and therefore the polymer matrix contains links and separate conductive particles. At high electric field the separated conductive particles may have electrostatic capacity, and thus the conductive particles may charge as in the circuit in Figure 5(b). The positively charged conductive particle may generate Coulomb attractive forces among the separated particles and repulsive forces among the linking particles and thus resistance may decrease and/or may increase. This can be explained as follows: the charge carriers in the sample move easily to the positive electrode and therefore the resistance in that side decreases. On the other hand, the carrier's vacancy concentration increases at the negative potential pole, resulting in an increasing resistance. Thereby, we conclude that the decrease of current is clearly generated by a repulsive force at high applied potential in the rubber matrix.[16,17] Furthermore, the temperature increases with increasing B_4C content in the composites. Another argument indicates that the thermal stability of the composites is enhanced by increasing filler content.

In Figure 5(a) the $(T_m - V)$ curve can be fitted by the empirical formula

$$T_s = \frac{T_N + (T_m - T_N)\left(\frac{V}{V_1}\right)^n}{1 + \left(\frac{V}{V_1}\right)^n} \tag{27}$$

where T_s is the equilibrium self-heating temperature at which the self-heating and heat dissipation are in balance; T_N and T_m are the room and maximum temperature, respectively; and V_1 is the applied voltage at which $T_s = T_N + 0.5(T_m - T_N)$. The parameter n is a power that makes the curve σ-shaped. From eq. (27), we can obtain the boundary conditions $T_s|_{V\to 0} = T_N$ and $T_s|_{V\to\infty} = T_m$.

With the experimental data in Figure 5(a) fitted into eq. (27), we calculated the values of V_1 and n with various initial resistances (R_0). The relationship between V_1 and R_0 can be described as

$$V_1 = N_D R_0^E \tag{28}$$

Least-squares fitting gives $E = 0.21$ and $N_D = 2.31$. The relationship between n and R_0 can be described by the power law

$$n = 4.05 R_0^{-0.051} \tag{29}$$

From eqs. (27), (28), and (29), we can draw a set of theoretical self-electrical heating, as shown in Figure 6, because these composites with various R_0 values may be very useful for planning groups in industrial applications of NTCC/PTCC thermistors.

Endurance test under applied power

An important issue in the production of conductive composites for self-electrical heating is the stability. Therefore, the NTCC/PTCC thermistors will have practical applications only when we can find solutions to the stability and reproducibility during thermal cycles and specified power cycles. To confirm the re-

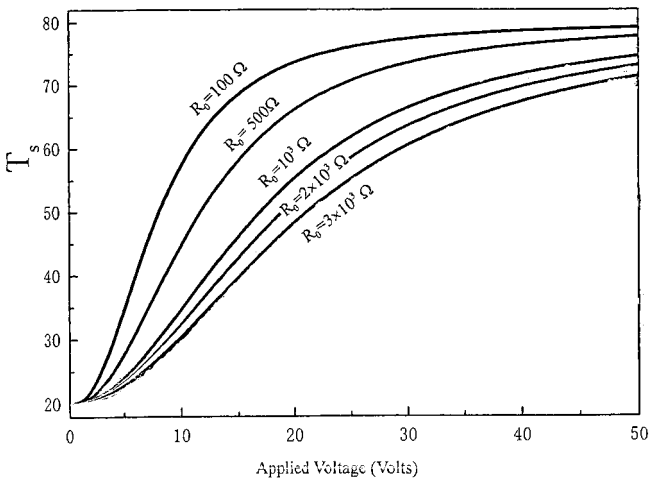

Figure 6 Set of plots of theoretical self-electrical heating (voltage–temperature) with various R_0 values of IIR/B_4C composites.

liability of the self-resetting performance, we carried out an endurance test with repeated thermal cycles under certain applied power. Furthermore, the response of the characteristics of temperature to an applied power is another important property to be examined for the NTCC composites being considered as an electrically self-heating probe/sensor. For this perspective, responses of $(T - I - t)$ to a certain applied power on and off for several cycles were obtained for sample F40 at am applied power of 3 W/cm^3, as shown in Figure 7. It is clear that the optimum temperature did not change with repeated power cycles (i.e., reversible behavior) for sample F40. This argument indicates that the B_4C particles improved the thermodynamic stability and molecular structure of the rubber matrix.

Modeling for evaluation of specific heat and heat transfer

The specific heats of rubber composites are very important for determining the life service of the final products under repeated stressing conditions. To calculate some useful thermal parameters such as the specific heat (C_p) and the amount of heat transferred by radiation and convection (H_r), the bulk temperature attributed to Joule heating (i.e., under applied potential) of the rubber samples was displayed as a function of time during the application of electric power across the sample. During measurement the initial applied power was kept constant at about 3 W/cm^3 up to attaining equilibrium temperature. Then C_p and H_r can be calculated using the following three models: (1) conservation law of energy, (2) Newton's law of cooling, and (3) adiabatic model.[13] In fact, after application of applied voltage on the sample, its temperature T increases with time t and the change dT in time dt is given by the following energy conservation equation:

$$RI^2\,dt = H_rS(T - T_1)\,dt + M_sC_{p(\mathrm{Cons})}\,dT \quad (30)$$

where R, M_s, $C_{p(\mathrm{Cons})}$, T_1, S, and H_r are electrical resistance, mass, specific heat, initial temperature, cross-sectional area of the sample, and amount of heat transfer, respectively.

The $(t - T)$ curve (Fig. 7) shows a thermal growth behavior and after a certain time levels off (i.e., equilibrium regime). The thermal growth regime can be described by the following empirical formula:

$$\left(\frac{T - T_1}{T_2 - T_1}\right) = (1 - e^{t/\tau_g}) \quad (31)$$

where T_2 is the maximum temperatures and τ_g is the thermal growth time constant, depending on B_4C content and is determined at $t = \tau_g$.

At thermal equilibrium regime (i.e., $dT = 0$) the amount of all heat transfers including heat transfer by radiation and convection are given by:

$$RI^2 = H_rS(T_2 - T_1) \quad (32)$$

The dependency of conduction current on time in Figure 7 can be expressed by the following equation:

$$\left(\frac{I_t - I_0}{I_m - I_0}\right) = \exp\left(-\frac{t}{t_i}\right) \quad (33)$$

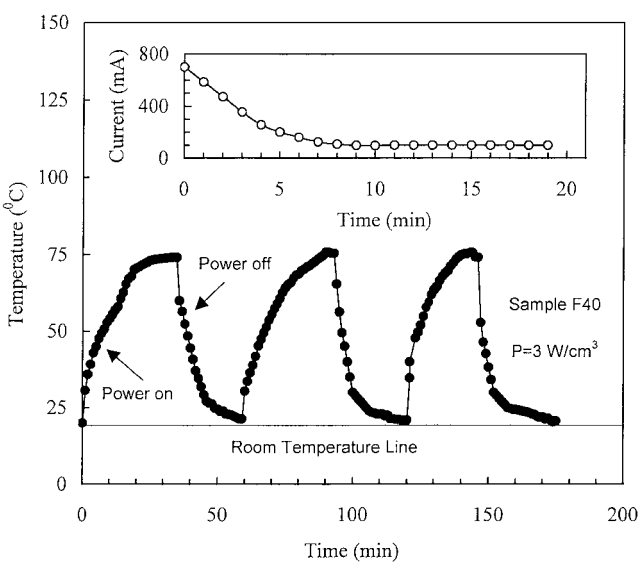

Figure 7 Response of $(T - I - t)$ to a certain applied power on and off for several cycles for sample F40 at applied power of 3 W/volume.

where t_i is a decay current constant (in s) and depending on B_4C content.

From eqs. (30)–(33) we get $C_{p(\text{Cons})}$ as the following:

$$RI^2 \int_{t_0}^{t_c} dt = H_r S(T - T_1) \int_{t_0}^{t_c} dt + M_s C_{p(\text{Cons})} \int_{T_0}^{T_m} dT \quad (34)$$

By integrating eq. (34) we get $C_{p(\text{Cons})}$ in the form

$$C_{p(\text{Cons})} = \left[\frac{1}{M_s(T_2 - T_1)}\right][V_0 t_m (T_2 - T_1)] + \ln\left(\frac{t_m + t_0}{t_0}\right) + V_0 I_m t_m - SH_r(T_2 - T_1)(t_m - e^{-(t/\tau_g)}) \quad (35)$$

On the other hand, if the thermistor has a uniform temperature during cooling (i.e., power off) the following equation is valid for the cooling of an NTCC in the time interval dt and according to Newton's law of cooling:

$$-C_{p(\text{Newt})} M_s \, dT = H_r(T_2 - T_1) \, dt \quad (36)$$

The solution of this equation for any value of t is

$$(T - T_1) = (T_3 - T_1)\exp\left(-\frac{t}{\tau_c}\right) \quad (37)$$

where T_3 is the temperature when time $t = 0$ and τ_c is the cooling constant in seconds.

From eqs. (36) and (37) we obtain $C_{p(\text{Newt})}$ in the form

$$C_{p(\text{Newt})} = \left(\frac{H_r \tau_c}{M_s}\right)(1 - e^{-(t/\tau_c)}) \quad (38)$$

According to the adiabatic model the $C_{p(\text{Adiab})}$ is given as[3]

$$C_{p(\text{Adiab})} = \frac{t_p RI^2}{M_s(T_2 - T_1)} \quad (39)$$

where t_p is the interval time to change the sample temperature from T_1 to T_2.

The estimated values of τ_g, τ_c, and τ_i as a function of B_4C content for IIR composites are listed in Table III, from which it may be seen that τ_g, τ_c, and τ_i decrease with increasing B_4C content, which increases the crosslinking density in the rubber matrix. This evidence affirms that B_4C enhances the inner structure of the rubber matrix, thus rendering it more thermodynamically stable. The experimental and calculated values of C_p by different models and the calculated values of H_r versus B_4C contents are listed in Table III, from which one may observe the slight difference between the sets of the calculated and experimental values, which suggests the reliability of the data. The values that were calculated for C_p are consistent with those reported in the literature.[3,13] The C_p and H_r values increase concomitantly with the increase of B_4C contents. This confirms that the inclusion of B_4C particles enhanced the inner morphology and connectivity among conductive particles in the IIR matrix, which is verified to be satisfactory in practical use as a self-electrical heating component.

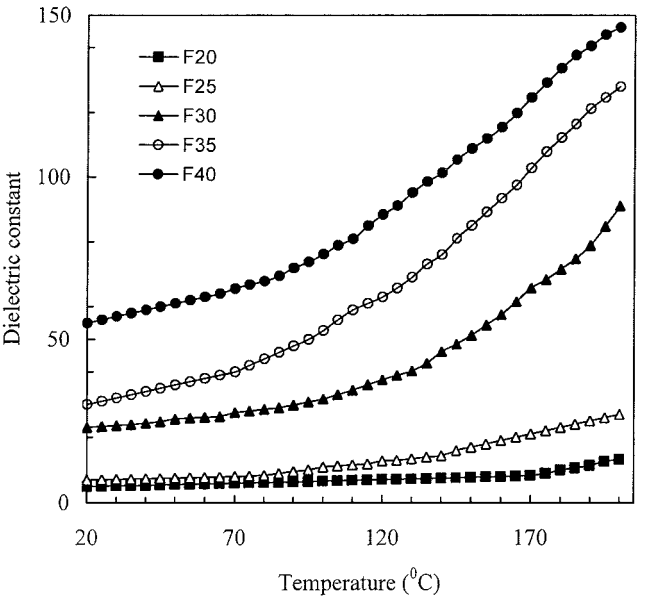

Figure 8 Variations of dielectric constant with temperature of IIR/B_4C composites.

Dielectric constant (ϵ) dependency on temperature

It is well known that the dielectric constant of a material arises because of the polarization of molecules and increases with increase in polarizability. The variations of dielectric constant at 1 kHz with temperature of IIR/B_4C composites are plotted in Figure 8, from which it may be observed that the dielectric constant values increase with the increase of B_4C contents at room temperature. This can be attributed to two phenomena: (1) morphological aspect changes with loading filler (i.e., the conductive phases become well dispersed and continuous with the increase of filler contents), which leads to an increase in ϵ; (2) the number of charge carriers increases with the loading of B_4C, which leads to an increase in the extent of orientational dipoles into the rubber matrix.[14] Therefore the increase in the value of ϵ is attributed to the interfacial polarization effects between filler and matrix. In Figure 8 it is clear that the ϵ increases gradually with the

increase of temperature because, at high temperature, both crosslinking and scission reactions operate.[2] We believe that if some scission predominates at high temperature, the rubber undergoes a dilation effect and chain fractures lead to entanglement couplings that then act as a crosslink. This tends to increase the effective dipole moment and the dielectric relaxation into the composite. Thus the dipole orientation increases and the interfacial area increases with the increase of temperature, which further leads to an increase of ϵ.

Thermal conductivity (λ) and thermal diffusivity (K_d) temperature dependency

Thermal conductivity and diffusivity are transport coefficients, related to the microscopic transport of heat, that depend on temperature, pressure, and, in the case of composites, on the filler content.[2] Typical values of λ and K_d versus temperature for IIR/B_4C composites are displayed in Figure 9(a) and (b), respectively. It may be clearly observed that both λ and K_d increase with the increase of B_4C contents, which suggests that λ and K_d of the composites depend significantly on the B_4C fractions in the composites. The increase in the λ and K_d values of composites with the increase of B_4C contents could be attributable to greater stability of the thermal conductive paths and stable interface between filler and matrix, which consequently reduce phonon scattering. Another possible reason is an increase of interfacial areas of the filler. The interfacial area can be viewed as a stable structure in which the conductive particles are well connected at the interface, thus becoming more effective in forming heat-conduction "net bridges" to transfer heat through the sample; this usually causes reduced diffusion of scattering phonons. It is seen that λ and K_d increase nonlinearly with the increase of temperature. It may be that with the increase of temperature, the interfacial area and interfacial resistance increase within the composites.[17,18] This leads to a considerable increase in the carrier mean free path and results in increasing the value of both λ and K_d. According to the aforementioned factors, the conduction mode that dominates λ and K_d of the composite is believed to be a combination of interface adhesion and volume fraction of filler.

However, the value of the figure of merit (Z) is defined as

$$Z = \frac{\sigma(TEP)^2}{\lambda} \tag{40}$$

The estimated values of Z as a function of B_4C content are listed in Table III. These results show that the Z value increases with B_4C content. This argument confirms that the incorporation of B_4C into the IIR matrix enhances their thermodynamic stability and network density.

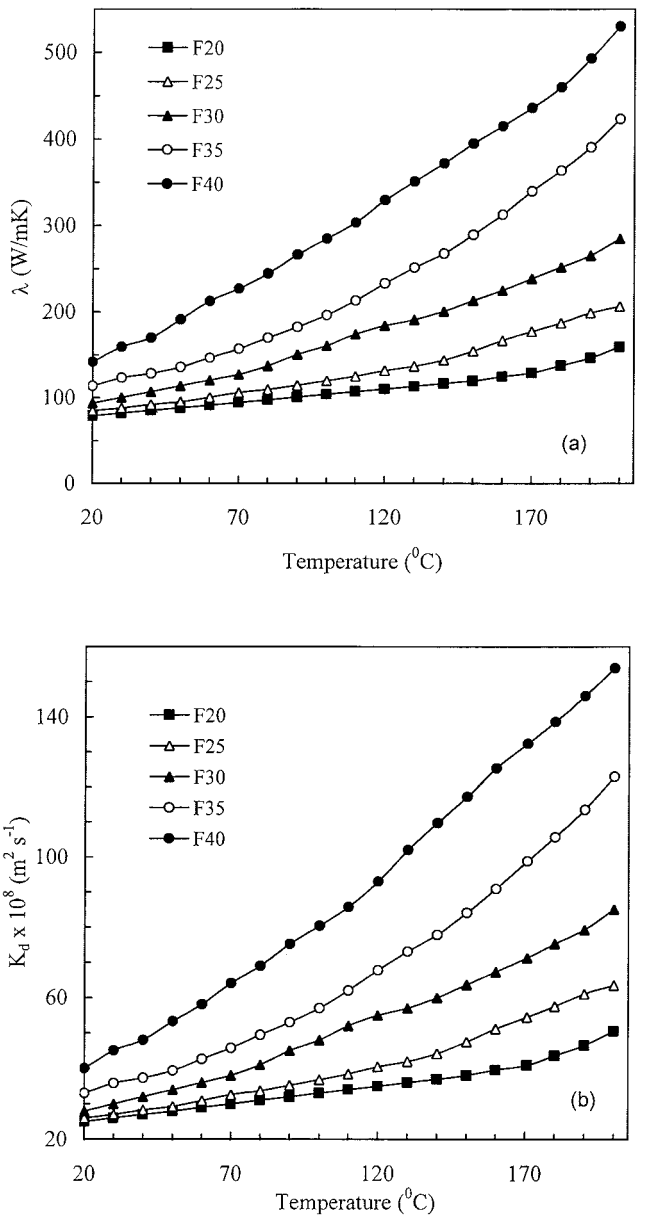

Figure 9 (a) $\lambda - T$ of IIR/B_4C composites; (b) $K_d - T$ of IIR/B_4C composites.

Electromagnetic wave shielding effectiveness (EMI)

For composites with polymeric matrix, EMI can be calculated from the electrical resistivity ρ of the composite as follows:

$$\text{EMI} = R + A + B \tag{41}$$

where R, A, and B are the reflection, absorption, and multireflection loss of the energy of the electromagnetic wave, respectively.

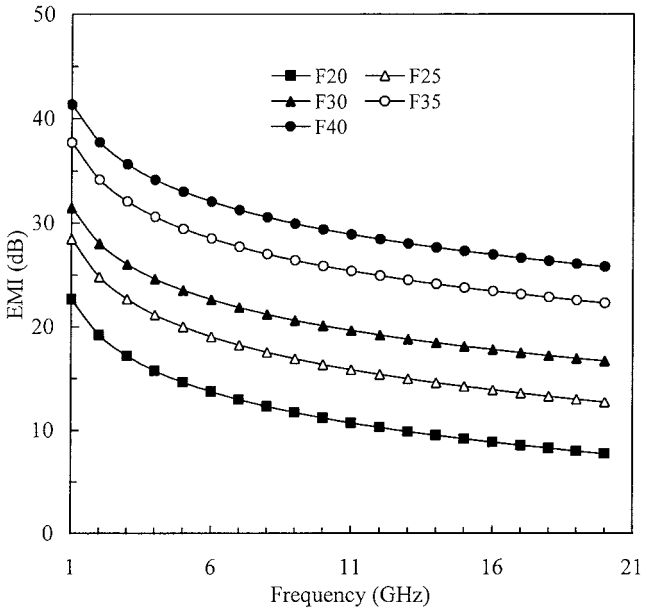

Figure 10 Theoretical relationship between EMI and the incidental frequency of the electromagnetic wave of IIR/B_4C composites.

The reflection loss is given by

$$R = 50.51 + 10 \log\left(\frac{1}{\mu f \rho}\right) \tag{42}$$

where μ is the magnetic permeability of the sample relative to vacuum and f is the incidental frequency of the electromagnetic wave (Hz) and

$$A = h \times 1.73 \sqrt{\frac{f}{\mu \rho}} \tag{43}$$

where h is the thickness of the composite.

The skin depth (SD) of electromagnetic radiation is given by

$$\mathrm{SD} = \frac{1}{\sqrt{\pi f \mu \sigma}} \tag{44}$$

The theoretical relationship between EMI and f of IIR/B_4C composites is presented in Figure 10. It is seen that the EMI is shown to be relatively frequency-dependent and EMI increases with an increasing B_4C content in the matrix. This is attributed to the formation of conductive network increases with increasing filler content as confirmed by the values of skin depth (SD) in Table IV. The estimated value of reflection loss is very high compared to the values of absorption loss, which implies that the EMI of IIR composites is attributable to the reflection loss at the surface.

The experimental parameters of EMI of IIR composites such as standing wave reflection (SWR), reflection coefficient, return loss, and attenuation are listed in Table IV It is seen that the return loss decreases with increasing B_4C content, which is ascribed to the high mobility carriers (i.e., composite changes from insulator to conductor phase) with the increase of B_4C content. The attenuation also increases with increasing B_4C content. This may be a result of the high interaction between filler and electromagnetic wave, which indicates that the EMI became more attenuated as the

TABLE IV
Experimental Values of Electromagnetic Wave Shielding Versus B_4C Content

Sample code	Frequency (GHz)	Standing wave ratio (SWR)	Reflection coefficient	Return loss, LR (dB)	Attenuation, Li (dB/cm)
F20	1.00	1.284	0.124	−18.69	2.545
	2.80	2.040	0.342	−9.218	8.862
	3.35	2.537	0.434	−7.721	11.650
	4.00	2.725	0.471	−7.420	12.500
F25	1.00	1.270	0.129	−18.460	3.325
	2.80	1.915	0.320	−8.660	7.570
	3.35	2.011	0.410	−7.200	6.897
	4.00	2.115	0.430	−7.000	9.315
F30	1.00	1.320	0.138	−17.202	3.729
	2.80	1.857	0.300	−7.720	9.370
	3.35	2.150	0.365	−6.590	7.875
	4.00	2.285	0.390	−6.350	10.620
F35	1.00	1.300	0.130	−17.690	4.560
	2.80	1.915	0.320	−8.315	10.540
	3.35	2.238	0.390	−6.940	9.150
	4.00	2.395	0.410	−6.650	9.750
F40	1.00	1.296	0.129	−16.681	7.350
	2.80	2.050	0.346	−7.238	12.060
	3.35	2.350	0.403	−5.93	9.747
	4.00	2.500	0.429	−5.641	10.150

σ and ϵ values increased. We concluded that the return losses and attenuation can be controlled with the content of B_4C in the rubber matrix.

CONCLUSIONS

The following conclusions may be drawn from this study.

1. The IIR/B_4C composite is a new prospective self-electrical heating composite with double (NTCC/PTCC) effect (i.e., V-shaped thermistor) and good for electromagnetic properties applications like enclosing computers, electronic devices, and microwave shielding.
2. The incorporation of B_4C into the rubber matrix increases the driving force of vulcanization and enhances the network structure density of the composites.
3. The IIR/B_4C composites exhibit linear conductivity behavior that could be controlled using B_4C particles for any desirable utilization technology. The thermoelectric power and power factor of IIR/B_4C composites is high, which make these composites potential candidates for improving the efficiency of thermoelectric devices and electrical energy conversion.
4. Electrical conductivity temperature dependency shows V-shaped effect (i.e., double NTCC/PTCC effect). The conduction mechanism of the composite is controlled by tunneling mechanism and behaves as a p-type semiconductor. Isothermal resistance relaxation with time at various temperatures for IIR/B_4C composites was investigated and results indicate that the interfacial adhesion and connectivity within the rubber matrix increases with increase of B_4C content.
5. Current–voltage dependency shows a certain kind of switch effect that makes these composites attractive for overcurrent-protection devices. It was also confirmed that the IIR/B_4C composite has good endurance and can be used instead of fuse-links in low-voltage circuits.
6. For many technical applications, the specific heat of rubber composite can be calculated with a simple conservation law of energy, which is in sufficient agreement with experimental data. Dielectric constant, thermal conductivity, and diffusivity all increase with the increase of filler and temperature because of the increase of the crosslinking density and interfacial adhesion.
7. EMI values of conductive IIR/B_4C composites are strongly dependent on filler fractions and frequency. The obtained composites have high attenuation and return loss values, and can be considered as advanced semiconductor materials for EMI applications.

References

1. El-Tantawy, F.; Kamda, K.; Ohnba, H. J Appl Polym Sci 2003, 87, 97.
2. El-Tantawy, F. Polym Degrad Stab 2001, 73, 289.
3. El-Tantawy, F. In: Proceedings of the 7th Japan International SAMPE Symposium and Exhibition, November 13–16, 2001; Tokyo, Japan; p. 797.
4. El-Tantawy, F.; Kamda, K.; Ohnba, H. Polym Int 2002, 51, 635.
5. Dishovsky, N.; Grigorova, M. Mater Res Bull 2000, 35, 403.
6. Song, Y. K.; El-Tantawy, F. Macromol Res 2003, 10, 126.
7. Krupa, I.; Chodak, I. Eur Polym J 2002, 37, 2159.
8. Tao, X.; Pan, Y.; Zheng, Q.; Yi, X. J Appl Polym Sci 2001, 79, 2258.
9. Ramani, R. Eur Polym J 1997, 33, 1753.
10. George, S.; Knoregen, M.; Thomus, S. J Membr Sci 1999, 1, 163.
11. Aminbahavi, T. M.; Harlapur, S. F.; Ortego, J. D. Polym Test 1997, 16, 91.
12. Breuer, O.; Narkis, M. J Appl Polym Sci 1999, 73, 1655.
13. Zhang, X. W.; Pan, Y.; Yi, Y. J Appl Polym Sci 2000, 78, 424.
14. George, S.; Varughese, K. T.; Thomas, S. J Appl Polym Sci 1999, 73, 255.
15. Hassan, H. H.; Abdel-barry, E. M.; Shash, N. M. Appl Phys Commun 1989, 9, 267.
16. Annadura, P.; Mallick, A. K.; Tripathy, D. K. J Appl Polym Sci 2002, 83, 145.
17. Werheit, H. Mater Sci Eng B 1995, 19, 228.
18. Zhang, X. W.; Pan, Y.; Yi, Y. J Appl Polym Sci 2000, 77, 756.